Response of Tropical Precipitation Extremes to Walker Circulation Strength in Warming Climates

Monica Caparas

December 2017

Abstract: Global warming is expected to lead to changes in the global hydrological cycle, including an intensification of precipitation extremes. Physically, changes in precipitation extremes with climate depends on changes in the moist-adiabatic temperature lapse rate, the upward velocity, and the temperature when they occur. In the tropics, the Walker Circulation is intimately tied to upward velocity and the El Niño Southern Oscillation (ENSO), which drives and depends on the sea surface temperature (SST) asymmetry across the tropical Pacific. How the Walker Circulation strength will change with global warming has been disputed in literature. Using an idealized aquaplanet general circulation model to isolate ocean-atmosphere dynamics, we simulate various Walker Circulation strengths by prescribing levels of zonally asymmetric ocean heat flux divergence (0, 20, 40, and 60 W/m^2) in a slab ocean configuration. Each level of Walker Circulation strength is forced under a climate scenario similar to present-day and then under incremental warming scenarios. We show that while precipitation extremes will intensify with both Walker Circulation strengthening and global warming, global mean precipitation does not change with Walker Circulation strengthening, and increases with global warming. The SST gradient in the tropics increases with Walker Circulation strengthening, but generally decreases with global warming. If the Walker Circulation strengthens under global warming, tropical precipitation extremes intensify in both frequency and magnitude. The changing of precipitation extremes to global warming, Walker Circulation strength, and SST gradient calls for further studies of the physical mechanisms behind responses of the Walker Circulation and ENSO to climate change.

1 Introduction

Motivation for Work

It is certain that warming from greenhouse gases will affect the global hydrological cycle by increasing atmospheric water vapor content by 8% per degree warming (Trenberth, 1999). However, global mean precipitation will increase more slowly at a rate of 1-2% per degree warming due to limitations on radiative atmospheric energy availability (Held and Soden, 2006; Stephens and Ellis, 2008). Where precipitation will increase is of the most interest to us— particularly over the tropical ocean. Together, the El Niño Southern Oscillation (ENSO) and the Walker Circulation largely affect tropical precipitation with ENSO variability being the strongest determining factor (Roeckner et al., 1996; McPhaden et al., 2006). However, there is disagreement of the direction of projected Walker Circulation strength with global warming (Merlis and Schneider, 2011; L'Heureux et al., 2013; Kociuba and Power, 2015; Zhang and Li, 2014). ENSO and the Walker Circulation drive and depend on sea surface temperatures (SST) in the equatorial Pacific Ocean and the SST gradient across the Pacific. Again, there is disagreement of projected SST gradient changes within model predictions and recent observational data (Deser et al., 2010; Zhang and Karnauskas, 2017). The strength of the Walker Circulation produces conditions similar to the two phases of ENSO—El Niño and La Niña—and affects the regional precipitation within the tropics. The aspect of tropical precipitation we investigate is extreme precipitation as climate models suggest extreme precipitation will increase more than mean precipitation under increased greenhouse gases (Pall et al., 2007). Understanding extreme precipitation is also a key aspect of understanding climate

impacts on society; however, extreme precipitation is underestimated within climate models compared to observations (Allan and Soden, 2008; Min et al., 2011). While extreme precipitation is not simulated reliably within models, upward velocity plays an important role in simulating extreme precipitation (O'Gorman and Schneider, 2009). Because upward velocity in the tropics is controlled by Walker Circulation strength, we simulate various strengths of the Walker Circulation in warming climates to analyze the response of extreme precipitations to this forcing. Before delving into our methodology and the model used, the driving motivations of this project—Walker Circulation, ENSO, and the global hydrological cycle and their responses to global warming— are explained in greater detail in the following sections.

Walker Circulation: Physical Mechanisms & History

The Walker Circulation is a zonal wind circulation system characterized by upward motion in the Western Pacific and downward motion in the Eastern Pacific. The branch of ascending air is characterized by a region of low-level convergence that drives convection, usually localized over warm water. After rising to higher altitudes, air in the upper troposphere flows from west to east before sinking to the surface in the Eastern Pacific, creating the descending branch of the Walker Circulation. Warm and moist air is transported by upward motion, while cool and dry air is transported by downward motion. Air at the surface is driven by easterly trade winds, flowing from east to west. The western branch of rising air and eastern branch of sinking air can deepen due to SST anomalies strengthening or weakening the SST gradient. Thus, SSTs in the equatorial Pacific are a main driving force of Walker Circulation strength (Kociuba and Power, 2014).

As the atmospheric branch of ENSO, the Walker Circulation is intimately tied to the Southern Oscillation, an atmospheric pressure pattern spanning the tropical Indian and Pacific Oceans. By observing sea level pressure and rainfall at centers around the globe, Sir Gilbert Walker recognized a seesaw pattern in sea level pressure between high pressure in the southeast Pacific Ocean and low pressure in the Indian Ocean (Walker, 1924; Rasmusson and Wallace, 1983). Following his discovery, scientists developed indices to measure the variability of Southern Oscillation as well as its teleconnectivity. Showing the strongest negative correlations of annual mean pressure between Darwin, Australia, and Tahiti in the south-central Pacific, the sea level pressure difference between Darwin and Tahiti established itself as the standard index for the Southern Oscillation (Trenberth, 1984; Ropelewski and Jones, 1984; Trenberth and Caron, 2000). Because sea level pressure drives surface winds, the Southern Oscillation and the Walker Circulation are two intimately tied phenomenon in the tropical Pacific Ocean that form ENSO (Julian and Chervin, 1978).

El-Niño Southern Oscillation (ENSO): Physical Mechanisms & Phases

ENSO is a coupled ocean-atmospheric phenomenon whose phases are determined by SST fluctuations. Though physically localized to the tropical Pacific, the cycling of ENSO phases largely influences on global weather patterns. ENSO variation is the most prominent year-to-year climate variation on Earth (McPhaden et al., 2006). The two phases of ENSO—El Niño and La Niña—recur every 2 to 7 years and develop with shifts in atmospheric and sea level pressure associated with surface wind strength, and thus are intimately tied to Walker Circulation (McPhaden et al., 2006). The ocean-atmosphere interactions that determine the conditions of Pacific Ocean are called the Bjerknes feedback, discovered by Jacob Bjerknes who linked the Southern Oscillation to ocean conditions during El Niño (Bjerknes, 1969). This positive feedback includes vertical motion in the atmosphere from surface to upper atmosphere, horizontal motion at the ocean-atmosphere interface across the Pacific, and vertical motion in the subsurface ocean.

We must consider the mean state of the tropical Pacific Ocean as a base foundation to describe the varying conditions of El Niño and La Niña. ENSO-neutral conditions show cooler SSTs in Eastern Pacific and warmer SSTs in the Western Pacific (Kessler, 2002). As part of the Bjerknes feedback, trade winds flow from east to west and pile warm surface water in the Western Pacific. Because surface water in the east is transported across the Pacific, upwelling beneath the surface brings colder water from deeper in the ocean to the surface in the eastern Pacific. This creates the

East-West SST gradient of cooler SSTs in Eastern Pacific and warmer SSTs in the Western Pacific that is observed as the mean state of the Pacific Ocean. The SST gradient reinforces the East-West pressure difference across the Pacific that drives the trade winds, completing the positive feedback cycle (McPhaden et al., 2006).

El Niño conditions reverse the Bjerknes feedback. The trade winds weaken, or possibly switch directions, and atmospheric pressure increases in the Western Pacific and decreases in the Eastern Pacific. Upwelling in the Eastern Pacific subsides. In the Eastern Pacific, anomalously warm SSTs can be observed from reduced upwelling and migration of warm surface water from the Western Pacific (McPhaden et al., 2006). The East-West SST gradient is reduced as SSTs across tropical Pacific are warmer than the mean, thus the East-West pressure difference that drives the trade winds is also reduced.

La Niña conditions amplify the Bjerknes feedback. The trade winds strengthen, atmospheric pressure decreases in the Western Pacific and increases in the Eastern Pacific, and upwelling in the Eastern Pacific intensifies. In the Eastern Pacific, anomalously cool SSTs can be observed from increased upwelling bringing colder subsurface water to the surface. The East-West SST gradient is stronger because SSTs in the eastern Pacific are cooler than the mean and SSTs in the western Pacific are warmer than the mean. Thus, the East-West pressure difference strengthens the trade winds.

Relationship between Tropical Precipitation, Walker Circulation, & Pacific SST gradient

Tropical precipitation is primarily controlled by Walker Circulation and ENSO, thus SSTs in the Pacific. During El Niño conditions when the SST gradient is weak, there is more precipitation in the central and Eastern Pacific and less precipitation in the Western Pacific. During La Niña conditions when the SST gradient is strong, there is more precipitation in the Western Pacific and less precipitation in the Eastern Pacific. Because of the conditions of trade wind strength and pressure difference across the Pacific, El Niño conditions are associated with a weaker Walker Circulation and La Niña conditions are associated with a stronger Walker Circulation—or, the SST gradient across the Pacific is linked to Walker Circulation strength (Meng et al., 2012). Thus, a weakened Walker Circulation is associated with a decrease in the SST gradient, or similar SSTs in both the Eastern Pacific and Western Pacific. Conversely, an intensified Walker Circulation is associated with an increase in the SST gradient, or anomalously warm SSTs in the Eastern Pacific and cool SSTs in the Western Pacific.

Responses of Walker Circulation & ENSO to Global Warming

There are discrepancies within literature of the response of the Walker Circulation to global warming in both model simulations and direct observations. The response of the Walker Circulation to global warming is extremely relevant because variations from the mean strength of the Walker Circulation influences weather and climate systems globally with the greatest effect on tropical weather and climate (Zhang and Li, 2017). Examination of future projections in climate models show a weakened Walker Circulation with future global warming (Held and Soden, 2006; Vecchi et al., 2006; Merlis and Schneider, 2011; Kociuba and Power, 2015; Zhang and Li, 2014). Examination of sea level pressure trends from 1900-2011 from ten different data sets drawn from reanalysis, reconstructions, and in situ measurements show a strengthened Walker Circulation with recent global warming (L'Heureux et al., 2013).

On the other hand, the wide natural variability of ENSO makes it difficult to discern internal variability from externally forced variability, such as increased variability due to global warming (Deser et al., 2012). Observational studies show El Niño and La Niña typically recurring every 2-7 years, showing an interannual variability in the ENSO cycling of its phases (McPhaden et al., 2006). However, looking on longer time scales, there is a residual component showing an interdecadal variability that differs in spatial conditions in SST, sea level pressure, and wind stress fields from the interannual variability (Zang et al., 1997; Chen and Wallace, 2015). There is an argument supported by direct observations that there have been more frequent, stronger El Niños than La Niñas since mid 1970s (McPhaden et al., 2006). However, climate models simulate a large range of ENSO behavior, and it is not well understood whether it is randomly generated, if other coupled

natural processes are dominant drivers of ENSO variability, or if an external force is the driving mechanism (Collins et al., 2010; Deser et al., 2010; Stevenson et al., 2012).

Using a coupled atmosphere-ocean model forcing warming and limiting atmospheric thermodynamics to only the effect of surface winds, Clement et al., (1996) proposed the effect of ocean dynamics on regulating tropical climate, introducing an "oceanic thermostat." Spatial differences in surface warming over the tropical ocean, heat flux out of anomalously warming regions, and vertical advection of heat through anomalous equatorial ocean upwelling affect atmospheric circulation. The addition of feedbacks, particularly ocean-atmosphere coupled feedbacks, would enhance the thermostat effect. Now it is nearly impossible to discuss tropical circulations like ENSO and the Walker Circulation without discussing the contributions of SST variation.

A noteworthy measure of change in both the Walker Circulation and ENSO is SST variability. Zhang and Li, (2017) examined the roles of three variations of SST warming on Walker Circulation changes to global warming: differential SST warming, uniform SST warming, and additional land warming. They found that differential SST warming amplifies weakening of the East-West SST gradient and Pacific trade winds, but because of this feedback, cannot be a fundamental cause the weakened Walker Circulation. Rather, uniform SST warming that affects the North Pacific Monsoon and land warming in South America attribute to the weakening of the Walker Circulation.

In addition to the complex spatial variability in responses of the Walker Circulation and ENSO to global warming, there is a temporal aspect of global mean response to radiative forcing that includes two components. Analysis of a coupled atmosphere-ocean general circulation model forced to preindustrial conditions and projected warming conditions decomposed the response to a fast component and a slow component (Held et al., 2010). The fast component responds to warming on a time scale of 5 years, and agreed with model simulations to be the dominant response to warming at the end of the twentieth century. On the other hand, the slow component has a sluggish growth response to warming with a different spatial structure than the fast component, holding significantly large variability in the responses of complex, coupled systems to warming.

Global Hydrological Cycle: Clausius-Clapeyron & Scaling

The 7% per degree increase in atmospheric water vapor content in response to global warming is largely governed by the Clausius-Claperyon equation

$$ln\frac{P_1}{P_2} = \frac{\Delta H_{vap}}{R}(\frac{1}{T_2} - \frac{1}{T_1}) \quad (1)$$

which is dependent on vapor pressure and temperature (Trenberth, 1999; Sun et al., 2007). This scaling with column water vapor content indicates that relative humidity remains roughly constant (Held et al., 2010; O'Gorman and Schneider, 2009). However, the increase in intensity of global hydrological cycle, or global mean precipitation, in response to global warming is far less than the Clausius-Clapyeron scaling— approximately 1-2% per degree warming (Cubasch et al., 2001). This is because the change in the intensity of the global hydrological cycle is controlled by surface energy availability rather than water vapor availability (Boer and Yu, 2003; Allen and Ingram, 2002; Stephens and Ellis, 2008).

Extreme Precipitation

Due to increased moisture convergence, intensification of extreme precipitation is an expected change in the global hydrological cycle in response to global warming (O'Gorman and Schneider, 2009; Allan and Soden, 2008). Changes in extreme precipitation are most impactful to societal well-being, and the magnitude of change is region-specific (Pfahl et al., 2017). Scaling of the response of extreme precipitation to global warming and whether or not it exceeds Clausius-Clayperon scaling depends on latitude. Particularly, changes in tropical precipitation extremes greatly exceed Clausius-Clayperon scaling (Sugiyama et al., 2010). In multi-model simulations, the Pacific Ocean warms more at the equator than at the subtropics, indicating greater changes in equatorial SSTs—the same SSTs that influence Walker Circulation and ENSO (Gastineau and Soden, 2009). Simulated in an atmospheric general circulation model, differential SST warming explains 63% of rainfall changes in the tropical Pacific under global warming (Zhang and Li, 2017). O'Gorman and

Schneider, (2009) proposed a scaling for extreme precipitation (P_e) based on changes in the moist adiabatic lapse rate ($\frac{dq_s}{dp}$), the upward velocity (ω_e), and the local temperature (T_e).

$$P_e \sim -\{\omega_e \frac{dq_s}{dp}|_{Te}\} \tag{2}$$

This scaling incorporates a dynamical aspect that is key to region-specific distribution of extreme precipitation, and, in the tropics, is intimately tied to the Walker Circulation (O'Gorman and Schneider, 2009; Pfahl et al., 2017).

2 Methods & Materials

Aquaplanet Model

To study the response of extreme precipitation to changes in atmospheric circulation and global warming, we use an idealized moist atmospheric general circulation model (GCM) similar to Frierson et al., (2007) and O'Gorman and Schneider, (2008). The model is an aquaplanet version of a Geophysical Fluid Dynamics Laboratory (GFDL) climate model. It excludes continental and topographical complexities that are present in the real world and treats the planet as a constant density, water-covered spherical ocean. We use a slab-ocean with 1-meter mixed layer as the boundary condition between ocean and atmosphere. The slab-ocean boundary takes into account radiative and turbulent surface flux exchange between the mixed layer of the ocean and the atmosphere. Using a gray-radiation scheme to represent longwave radiative transfer, atmospheric longwave fluxes are simplified. Broadband longwave fluxes are absorbed, ignoring water vapor and cloud radiative effects. Using an aquaplanet model simplifies atmospheric convective dynamics and isolates ocean-atmosphere dynamics.

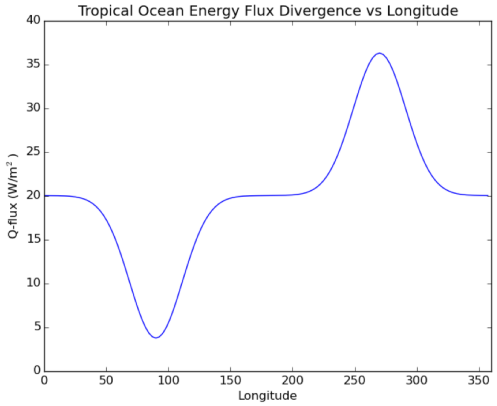

Figure 1: Prescribed ocean energy flux divergence (Q-flux) versus longitude averaged within -15° South to 15° North, for which increasing positive values indicate cooling tendencies and decreasing positive values indicate warming tendencies.

Simulations

The series of simulations ran under the model differ by variations of the Walker Circulation strength within global warming scenarios. How the Walker Circulation and global warming was represented in the model are described below.

Prescribed ocean energy flux divergence

Prescribing an ocean heat flux divergence (Q-flux), we simulate the Walker Circulation as Q-flux represents the influence of ocean circulation on surface temperature. Representing the divergence of the meridional ocean energy flux, a component of the Q-flux varies only in latitude and is mathematically represented as

$$\nabla \cdot F_o(\phi) = Q_o(\frac{1-2\phi^2}{\phi_o^2})exp(\frac{-\phi^2}{\phi_o^2}) \tag{3}$$

where ϕ is latitude, $\phi_o = 16°$, and Q_o= 50 W/m^2. Following Merlis and Schneider, (2011) and Bordoni and Schneider, (2008), the reference latitude ϕ_o is set to 16° and Q_o is set to 50 W/m^2.

Prescribed zonally asymmetric ocean energy flux divergence

Further following Merlis and Schneider, (2011), the zonally asymmetric component of the Walker Circulation is represented by adding and subtracting Gaussian lobes along the equator that are spaced 180 degrees longitude apart (Figure 1).

$$\begin{aligned}\nabla \cdot [F_o(\phi) + F_1(\lambda,\phi)] = \nabla \cdot F_o(\phi) + \\ Q_1 exp[-\frac{(\lambda-\lambda_E)^2}{\lambda_1^2} - \frac{(\phi^2}{\phi_1}] - \\ Q_1 exp[-\frac{(\lambda-\lambda_W)^2}{\lambda_1^2} - \frac{(\phi^2}{\phi_1}]\end{aligned} \tag{4}$$

Global warming:

	α=1.0	α=1.4	α=1.8
SST (K)	293	298	302
Mean Precipitation (mm/day)	4.55	5.14	5.46
Extreme Precipitation (mm/day)	35.1	40.9	46.1

Table 1: Global mean SST (K), global mean precipitation (mm/day), and tropical extreme precipitation (mm/day) at present-day Walker Circulation strength, or Q-flux= 40, for all climate cases, or α=1.0, 1.4, and 1.8.

where λ is longitude, $\lambda_1 = 30°$, $\lambda_E = 90°$, $\lambda_W = 270°$, $\phi_1 = 7°$, and $Q_o = 40$ W/m^2. Values of Q-flux are set to 0, 20, 40, and 60 W/m^2 to simulate various Walker Circulation strengths. Present-day conditions of the Walker Circulation are similar to Q-flux=40 W/m^2 case. From here on further, the variations of Walker Circulation strength are generally acknowledged as Q-flux variations. SST is one of the driving factors for Walker Circulation strength, and prescribing zonally asymmetric ocean energy flux divergence mimics the SST gradient. The resulting Q-flux has similar magnitude and spatial scale to reanalysis estimates (Trenberth et al., 2001; Merlis and Schneider, 2011).

Forced global warming

In a grey atmosphere scheme, global warming is forced by rescaling the alpha (α) parameter of the reference optical depth,

$$\tau = \alpha \tau_{ref} \tag{5}$$

where τ_{ref} is the reference optical depth that is a function of latitude and height (Merlis and Schneider, 2011). We use values of 1.0, 1.4, and 1.8 to simulate present-day climate at (α)=1.0 and approximately 5 K incremental warming with each increasing value. Global mean surface temperature ranges from 293 K to 302 K (Table 1). For each climate scenario, four cases for Q-flux are ran, resulting to a total of 12 simulations. Each simulation ran on a daily time scale, spun for 1200 days, and the last 800 days are analyzed.

Defining Extreme Precipitation

We define extreme precipitation as the 99.99^{th} percentile of precipitation in the tropics from -7° South to 7° North, consistent with O'Gorman and Schneider, (2009). The trends of intensity and frequency of extreme precipitation Walker Circulation strength is consistent among 99^{th}, 99.9^{th}, and 99.99^{th} percentiles.

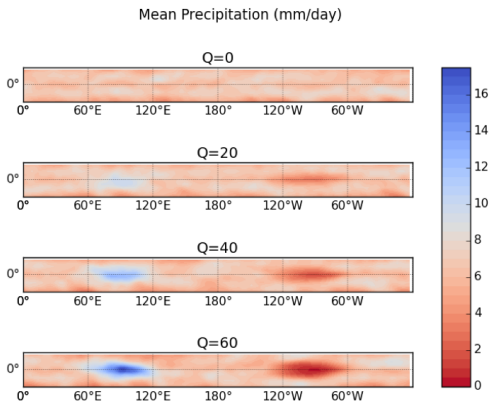

Figure 2: Contour plots of of time-averaged precipitation (mm/day) in the tropical region -15° South to 15° North for all Q-flux cases from α=1.0 case.

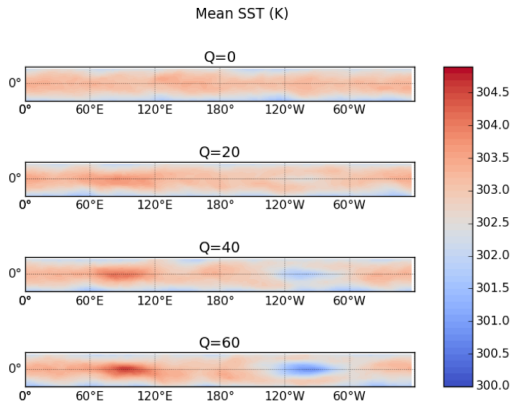

Figure 3: Contour plots of of time-averaged SST (K) in the tropical region -15° South to 15° North for all Q-flux cases from α=1.0 case.

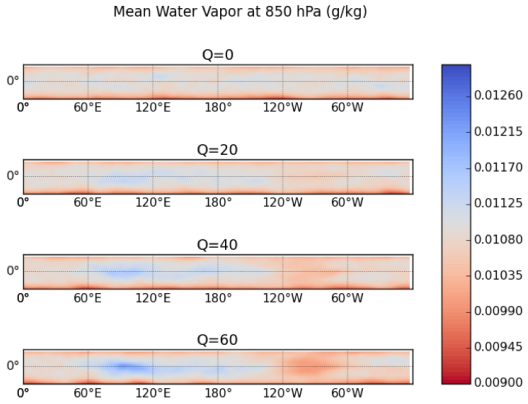

Figure 4: Contour plots of of time-averaged water vapor at 850 hPa (g/kg) the tropical region -15° South to 15° North for all Q-flux cases from α=1.0 case.

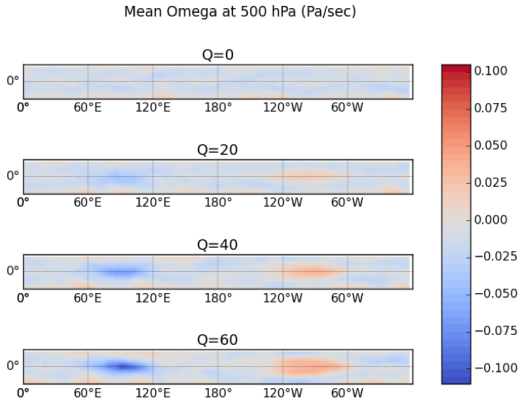

Figure 5: Contour plots of 500 hPa (Pa/sec) in the tropical region -15° South to 15° North for all Q-flux cases from α=1.0 case.

3 Results & Discussion

Regional Changes

Regional responses of mean precipitation, SST, water vapor, and omega (vertical velocity) vary to forced Walker Circulation strengthening. In present-day climate conditions (α=1.0 case), if Walker Circulation strengthens, mean SST and precipitation change in the same direction (Figures 2 and 3). In a west pool, or the ascending branch of the Walker Circulation, SST increases approximately 2 K and precipitation increases 14 mm/day from the no Walker Circulation case (Q-flux=0 W/m^2) to strongest Walker Circulation case (Q-flux=60 W/m^2). In an east pool, or the descending branch of the Walker Circulation, SST decreases approximately 3.5 K and precipitation decreases 6 mm/day from Q-flux=0 W/m^2 to Q-flux=60 W/m^2. The changes in SST and precipitation between the end-members of Walker Circulation strength supports the general statement: SST increases (decreases) where precipitation increases (decreases). This relationship between SST, precipitation, and Walker Circulation strength is consistent throughout global warming cases (α=1.4 and 1.8; not shown), supporting the "warmer becomes wetter" and "cooler becomes 'drier'" mechanism in the tropical ocean (Sun et al., 2007).

As expected, there is more atmospheric water vapor where there is more precipitation, and less water vapor where there is less precipitation (Figures 2 and 4). Comparing mean precipitation and water vapor at 850 hPa, water vapor increases approximately 0.001 g/kg to the 14 mm/day increase in precipitation in the ascending branch. Conversely, water vapor decreases 0.001 g/kg to the 6 mm/day decrease in precipitation in the descending branch. The change in water vapor to the change in mean precipitation with global warming is not a one-to-one relationship, as thoroughly reviewed in literature (Held and Soden, 2006;

Change in Walker Circulation Strength:

	Q-flux=0	**Q-flux=20**	**Q-flux=40**	**Q-flux=60**
SST (K)	293	293	293	293
Mean Precipitation (mm/day)	4.55	4.55	4.55	4.55
Extreme Precipitation (mm/day)	31.1	32.9	35.1	39.1

Table 2: Global mean SST (K), global mean precipitation (mm/day), and tropical extreme precipitation (mm/day) at all Walker Circulation strengths, or Q-flux= 0, 20, 40, and 60 W/m^2, for present-day climate, or α= 1.0.

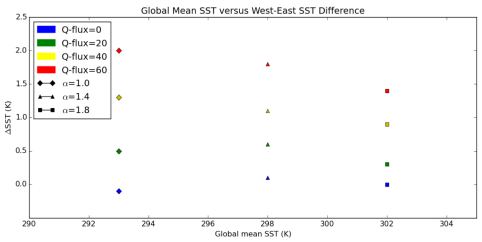

Figure 6: Global mean SST (K) versus West minus East SST difference (K) for all Walker Circulation strengths, or all Q-flux cases, from all climate scenarios, or all α simulations.

Stephens and Ellis, 2008). Under forced increasing Walker Circulation strength, the indirect relationship between water vapor and precipitation indicates that there are other additional factors driving precipitation changes in the tropics.

Unlike the relationship between SST and precipitation, omega at 500 hPa, or vertical velocity, and precipitation in the tropics change in opposing directions when Walker Circulation forced (Figures 2 and 5). That is, vertical velocity decreases (increases) where precipitation increases (decreases). Negative vertical velocity values signify upward motion and more convection, and positive vertical velocity values signify downward motion and less convection. In the ascending branch of the Walker Circulation, vertical velocity decreases approximately 0.1 Pa/sec. In the descending branch of the Walker Circulation, vertical velocity increases between 0.03-0.05 Pa/sec. Where there is more upward motion, there is more precipitation. Where there is more downward motion, there is less precipitation. In addition to magnitude change, there appears to be a small region of strong convection in the west pool and zonal spreading of weak convection in the east pool when Walker Circulation is forced to the highest strength (Q-flux=60 W/m^2).

Global Mean Precipitation

Extreme precipitation changes largely with Walker Circulation strengthening and with global warming, but mean precipitation changes only with global warming. Global mean precipitation remains constant when Walker Circulation strength is forced, indicating that the Walker Circulation does not affect global mean precipitation. Tropical extreme precipitation increases by 8 mm/day from the case with no Walker Circulation (Q-flux=0 W/m^2) to the strongest Walker Circulation case (Q-flux=60 W/m^2) (Table 2). Total SST and precipitation does not change with forced Walker Circulation strength across all climate cases. In increasing warming conditions, mean precipitation increases 2.6% per degree warming from α= 1.0 to α= 1.4 and 1.6% per degree warming from α= 1.4 to α= 1.8, consistent with changes in global

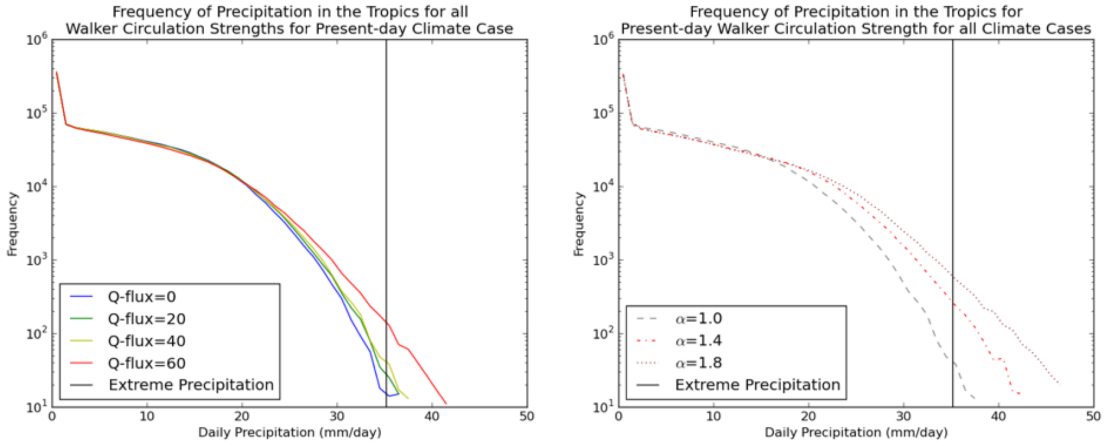

Figure 7: Frequency of daily precipitation (mm/day) for all Walker Circulation strengths, or Q-flux= 0, 20, 40 and 60 W/m^2, for present-day climate case, or α= 1.0 (left) and for present-day Walker Circulation strength, or Q-flux= 40 W/m^2 for all climate cases, or α= 1.0, 1.4, and 1.8 (right). Vertical solid line is the extreme precipitation value for Q-flux= 40 W/m^2 at α=1.0.

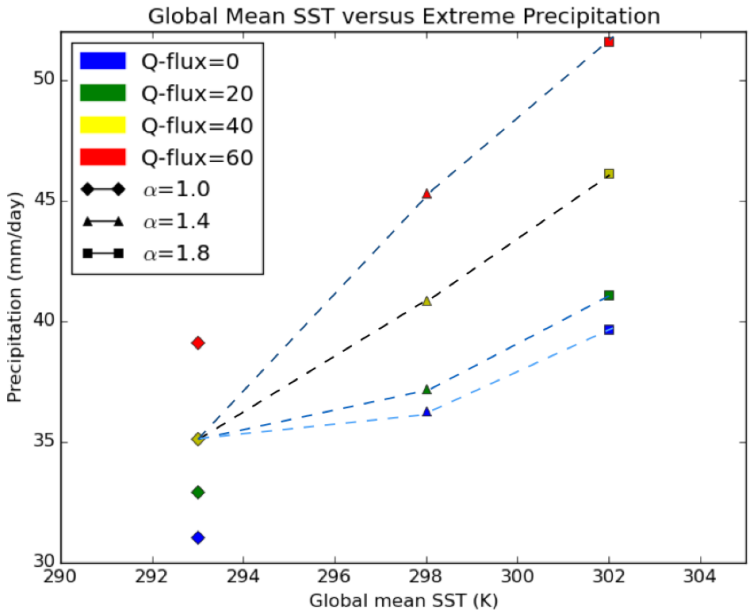

Figure 8: Global mean SST (K) versus extreme precipitation (mm/day) for all Walker Circulation strengths, or all Q-flux cases, from all climate scenarios, or all α simulations Lighter blue dashed lines indicate Walker Circulation weakening from present-day, darker blue dashed line indicates Walker Circulation strengthening from present-day, and black dashed line indicates no change in Walker Circulation strength from present-day.

mean precipitation due to warming. Under fixed Walker Circulation conditions similar to present-day strength (Q-flux= 40 W/m^2), global mean precipitation increases 0.91 mm/day with a 9 K increase in global mean SST while tropical extreme precipitation increases 11 mm/day (Table 1). This suggests the sensitivity of tropical extreme precipitation to warming is stronger than the sensitivity of global mean precipitation.

SST Gradient

Under each climate scenario, there is a greater West-East SST difference with increased Walker Circulation strength (Figure 6). When global mean SST is 293 K, or α=1.0, the SST gradient across the tropics increases when Walker Circulation strength increases, or when Q=flux increases from 0 to 60 W/m^2. This is consistent across warming scenarios, α=1.4 (global mean SST= 298 K) and α=1.8 (global mean SST= 302 K). Under global warming with fixed Walker Circulation strength, the SST gradient generally decreases. At present-day and stronger Walker Circulation conditions (Q-flux=40 and 60 W/m^2), the SST gradient decreases with increased global mean SST. At weaker and no Walker Circulation conditions (Q-flux=20 and 0 W/m^2), the SST gradient slightly increases from α=1.0 to α=1.4, then decreases from α=1.4 to α=1.8. The discrepancy from α=1.0 to α=1.4 is likely due to sensitivity to the computational definitions of 'West' and 'East' as West-East SST differences are very small or non-existent at weak Walker Circulation strength (Q-flux= 20 W/m^2) or no Walker Circulation at all (Q-flux= 0 W/m^2) (Figure 2). The general decrease in the SST gradient across the tropics with global warming is consistent with results from Merlis and Schneider, (2011).

Increased Frequency & Intensity

Extreme precipitation increases in frequency with Walker Circulation strengthening and global warming (Figure 7). Extreme precipitation becomes more frequent by a magnitude of 10^1 when Walker Circulation strength is forced under present-day climate conditions, and also by a magnitude of 10^1 when global warming is forced under present-day Walker Circulation strength.

Extreme precipitation in the tropics increases whether global mean SST increases and the Walker Circulation strengthens, but the magnitude of increased intensity of extreme precipitation depends on Walker Circulation strengthening or weakening with global warming (Figure 8). If Walker Circulation strength does not change with global warming, extreme precipitation still intensifies 7-14 mm/day. If Walker Circulation strength remains similar to present-day (Q-flux=40 W/m^2), extreme precipitation increases from 35 mm/day in present-day climate case (α= 1.0) to 46 mm/day in α= 1.8 warming case. The possible projected pathways of changes in Walker Circulation strength from present-day conditions clearly shows that changes in extreme tropical precipitation with global warming is determined by Walker Circulation strength.

4 Conclusion

Atmospheric dynamics, particularly the strength of the Walker Circulation, play a dominant role in tropical extreme precipitation, as supported by O'Gorman and Schneider, (2009). Under current climate, if the Walker Circulation strengthens, there will be a greater SST gradient and higher increase in intensity and frequency of extreme precipitation. Under global warming, if the Walker Circulation weakens, there will be a smaller SST gradient and lower increase in intensity and frequency of extreme precipitation. Conversely, if the Walker Circulation strengthens under global warming, there will be a greater SST gradient and higher increase in intensity and frequency of extreme precipitation. The strength of the Walker Circulation is a strong determining factor in the changes of tropical extreme precipitation and SST gradient in response to global warming.

References

Richard P Allan and Brian J Soden. Atmospheric warming and the amplification of precipitation extremes. *Science*, 321(5895):1481–1484, 2008.

Myles R Allen and William J Ingram. Constraints on future changes in climate and the hydrologic cycle. *Nature*, 419(6903):224–232, 2002.

Jakob Bjerknes. Atmospheric teleconnections from the equatorial pacific. *Monthly Weather Review*, 97(3):163–172, 1969.

GJ Boer and B Yu. Climate sensitivity and climate state. *Climate Dynamics*, 21(2):167–176, 2003.

Simona Bordoni and Tapio Schneider. Monsoons as eddy-mediated regime transitions of the tropical overturning circulation. *Nature Geoscience*, 1(8):515–519, 2008.

Xianyao Chen and John M Wallace. Enso-like variability: 1900–2013. *Journal of Climate*, 28 (24):9623–9641, 2015.

Amy C Clement, Richard Seager, Mark A Cane, and Stephen E Zebiak. An ocean dynamical thermostat. *Journal of Climate*, 9(9):2190–2196, 1996.

Mat Collins, Soon-Il An, Wenju Cai, Alexandre Ganachaud, Eric Guilyardi, Fei-Fei Jin, Markus Jochum, Matthieu Lengaigne, Scott Power, Axel Timmermann, et al. The impact of global warming on the tropical pacific ocean and el niño. *Nature Geoscience*, 3(6):391–397, 2010.

U Cubasch, GA Meehl, GJ Boer, RJ Stouffer, M Dix, A Noda, CA Senior, S Raper, and KS Yap. Projections of future climate change. *, in: JT Houghton, Y. Ding, DJ Griggs, M. Noguer, PJ Van der Linden, X. Dai, K. Maskell, and CA Johnson (eds.): Climate Change 2001: The Scientific Basis: Contribution of Working Group I to the Third Assessment Report of the Intergovernmental Panel*, pages 526–582, 2001.

Clara Deser, Adam S Phillips, and Michael A Alexander. Twentieth century tropical sea surface temperature trends revisited. *Geophysical Research Letters*, 37(10), 2010.

Clara Deser, Adam S Phillips, Robert A Tomas, Yuko M Okumura, Michael A Alexander, Antonietta Capotondi, James D Scott, Young-Oh Kwon, and Masamichi Ohba. Enso and pacific decadal variability in the community climate system model version 4. *Journal of Climate*, 25(8):2622–2651, 2012.

Dargan MW Frierson, Isaac M Held, and Pablo Zurita-Gotor. A gray-radiation aquaplanet

moist gcm. part ii: Energy transports in altered climates. *Journal of the atmospheric sciences*, 64(5):1680–1693, 2007.

Guillaume Gastineau and Brian J Soden. Model projected changes of extreme wind events in response to global warming. *Geophysical Research Letters*, 36(10), 2009.

Isaac M Held and Brian J Soden. Robust responses of the hydrological cycle to global warming. *Journal of climate*, 19(21):5686–5699, 2006.

Isaac M Held, Michael Winton, Ken Takahashi, Thomas Delworth, Fanrong Zeng, and Geoffrey K Vallis. Probing the fast and slow components of global warming by returning abruptly to preindustrial forcing. *Journal of Climate*, 23 (9):2418–2427, 2010.

William S Kessler. Is enso a cycle or a series of events? *Geophysical Research Letters*, 29(23), 2002.

Greg Kociuba and Scott B Power. Inability of cmip5 models to simulate recent strengthening of the walker circulation: Implications for projections. *Journal of Climate*, 28(1):20–35, 2015.

Michelle L L'Heureux, Sukyoung Lee, and Bradfield Lyon. Recent multidecadal strengthening of the walker circulation across the tropical pacific. *Nature Climate Change*, 3(6):571–576, 2013.

Michael J McPhaden, Stephen E Zebiak, and Michael H Glantz. Enso as an integrating concept in earth science. *science*, 314(5806):1740–1745, 2006.

Qingjia Meng, Mojib Latif, Wonsun Park, Noel S Keenlyside, Vladimir A Semenov, and Thomas Martin. Twentieth century walker circulation change: Data analysis and model experiments. *Climate dynamics*, 38(9-10):1757–1773, 2012.

Timothy M Merlis and Tapio Schneider. Changes in zonal surface temperature gradients and walker circulations in a wide range of climates. *Journal of Climate*, 24(17):4757–4768, 2011.

Seung-Ki Min, Xuebin Zhang, Francis W Zwiers, and Gabriele C Hegerl. Human contribution to more-intense precipitation extremes. *Nature*, 470(7334):378–381, 2011.

Paul A O'Gorman and Tapio Schneider. The physical basis for increases in precipitation extremes in simulations of 21st-century climate change. *Proceedings of the National Academy of Sciences*, 106(35):14773–14777, 2009.

Paul A O'Gorman and Tapio Schneider. The hydrological cycle over a wide range of climates simulated with an idealized gcm. *Journal of Climate*, 21(15):3815–3832, 2008.

Pardeep Pall, MR Allen, and Dáithí A Stone. Testing the clausius–clapeyron constraint on changes in extreme precipitation under co2 warming. *Climate Dynamics*, 28(4):351–363, 2007.

S Pfahl, PA O'Gorman, and EM Fischer. Understanding the regional pattern of projected future changes in extreme precipitation. *Nature Climate Change*, 7(6):423–427, 2017.

Erich Roeckner, Josef-M Oberhuber, Andreas Bacher, Michael Christoph, and Ingo Kirchner. Enso variability and atmospheric response in a global coupled atmosphere-ocean gcm. *Climate Dynamics*, 12(11):737–754, 1996.

Graeme L Stephens and Todd D Ellis. Controls of global-mean precipitation increases in global warming gcm experiments. *Journal of Climate*, 21(23):6141–6155, 2008.

Samantha Stevenson, Baylor Fox-Kemper, Markus Jochum, Richard Neale, Clara Deser, and Gerald Meehl. Will there be a significant change to el niño in the twenty-first century? *Journal of Climate*, 25(6):2129–2145, 2012.

Masahiro Sugiyama, Hideo Shiogama, and Seita Emori. Precipitation extreme changes exceeding moisture content increases in miroc and ipcc climate models. *Proceedings of the National Academy of Sciences*, 107(2):571–575, 2010.

Ying Sun, Susan Solomon, Aiguo Dai, and Robert W Portmann. How often will it rain? *Journal of Climate*, 20(19):4801–4818, 2007.

Kevin E Trenberth. Conceptual framework for changes of extremes of the hydrological cycle with climate change. In *Weather and Climate Extremes*, pages 327–339. Springer, 1999.

Kevin E Trenberth, Julie M Caron, and David P Stepaniak. The atmospheric energy budget and implications for surface fluxes and ocean heat transports. *Climate dynamics*, 17(4):259–276, 2001.

Gabriel A Vecchi, Brian J Soden, Andrew T Wittenberg, Isaac M Held, Ants Leetmaa, and Matthew J Harrison. Weakening of tropical pacific atmospheric circulation due to anthropogenic forcing. *Nature*, 441(7089):73–76, 2006.

Y Zang, JM Wallace, and DS Battisti. Enso-like interdecadal variability: 1900–1993. *Journal of Climate*, 10:1004–1020, 1997.

Lei Zhang and Kristopher B Karnauskas. The role of tropical interbasin sst gradients in forcing walker circulation trends. *Journal of Climate*, 30(2):499–508, 2017.

Lei Zhang and Tim Li. A simple analytical model for understanding the formation of sea surface temperature patterns under global warming. *Journal of Climate*, 27(22):8413–8421, 2014.

Lei Zhang and Tim Li. Relative roles of differential sst warming, uniform sst warming and land surface warming in determining the walker circulation changes under global warming. *Climate Dynamics*, 48(3-4):987–997, 2017.